

On Symmetry, Perspectivity and Level-set based Segmentation

Tammy Riklin-Raviv^a Nir Sochen^b Nahum Kiryati^c

^a Computer Science and Artificial Intelligence Laboratory, MIT

^b Department of Applied Mathematics, Tel Aviv University

^c School of Electrical Engineering, Tel Aviv University

Abstract

We introduce a novel variational method for the extraction of objects with either bilateral or rotational symmetry in the presence of perspective distortion. Information on the symmetry axis of the object and the distorting transformation is obtained as a by-product of the segmentation process. The key idea is the use of a flip or a rotation of the image to segment as if it has been another view of the object. We call this generated image the *symmetrical counterpart* image. We show that the symmetrical counterpart image and the source image are related by planar projective homography. This homography is determined by the unknown planar projective transformation that distorts the object symmetry.

The proposed segmentation method uses a level-set based curve evolution technique. The extraction of the object boundaries is based on the symmetry constraint and the image data. The symmetrical counterpart of the evolving level-set function provides a dynamic shape prior. It supports the segmentation by resolving possible ambiguities due to noise, clutter, occlusions and assimilation with the background. The homography that aligns the symmetrical counterpart to the source level-set is recovered via a registration process carried out concurrently with the segmentation. Promising segmentation results of various images of approximately symmetrical objects are shown.

Index Terms

Symmetry, Planar projective transformation, Segmentation, Level-sets

I. INTRODUCTION

Shape symmetry is a useful visual feature for image understanding [48]. This research employs symmetry for segmentation¹. In the presence of noise, clutter, shadows, occlusions or assimilation with the background, segmentation becomes challenging. In these cases, object boundaries do not fully correspond to edges in the image and may not delimit homogeneous image regions. Hence, classical region-based and edge-based segmentation techniques are not sufficient. We therefore suggest a novel approach to facilitate segmentation of objects that are *known* to be symmetrical, by using their symmetry property as a shape constraint. The model presented is applicable to objects with either rotational or bilateral (reflection) symmetry distorted by projectivity.

The proposed segmentation method partitions the image into foreground and background domains, where the foreground region is known to be approximately symmetrical up to planar projective transformation. The boundary of the symmetrical region (or object) is inferred by minimizing a cost functional. This functional imposes the smoothness of the segmenting contour, its alignment with the image edges and the homogeneity of the regions it delimits. The assumed symmetry property of the object to extract provides an essential additional constraint.

There has been intensive research on symmetry related to human and computer vision. We mention a few of the classical and of the most recent papers. Most natural structures are only approximately symmetrical, therefore there is a great interest, pioneered by the work of [56] and followed by [18], in defining a measure of symmetry. There is a mass of work on symmetry and symmetry-axis detection [1], [5], [19], [23], [29], [31], [34], [44], [49]. Recovery of 3D structure from symmetry is explored in [12], [42], [45], [46], [50], [53], [57]. There are a few works that use symmetry for grouping [43] and segmentation [13], [14], [25], [27], [54]. The majority of the symmetry-related papers consider either bilateral symmetry [12], [42], [57] or rotational symmetry [5], [16], [55], [34]. Some studies are even more specific, for example [30] suggests a symmetry measure for bifurcating structures, [17] handles tree structures and [16], [53] demonstrate the relation between symmetry and perspectivity on simple geometrical shapes.

Only few algorithms treat the symmetrical object shape as a single entity and not as a collection of landmarks or feature points. Refer for example to [44] that suggests the edge strength function to determine the axes of local symmetry in shapes, using variational framework. In the suggested

¹A preliminary version of this manuscript appeared in [37].

framework the symmetrical object contour is represented as a single entity by the zero-level of a level-set function. We assign, w.l.o.g., the positive levels to the object domain. Taking the role of object indicator functions level-sets are most adequate for dynamic shape representation. A dissimilarity measure between objects is defined as a function of the weighted sum of pixels with contradicting labeling. Transformation of the region bounded by the zero level is applied by a coordinate transformation of the domain of the embedding level-set function [38], as illustrated in Fig. 1.

We define the concept of *symmetrical counterpart* in the context of image analysis. When the imaged object has a bilateral symmetry, the symmetrical counterpart image is obtained by a vertical (or horizontal) flip of the image domain. When the imaged object has a rotational symmetry, the symmetrical counterpart image is provided by a rotation of the image domain. In the same manner we define the symmetrical counterpart of a level-set (or a labeling) function. The symmetry constraint is imposed by minimizing the dissimilarity measure between the evolving level-set (labeling) function and its symmetrical counterpart. The proposed segmentation approach is thus fundamentally different from other methods that support segmentation by symmetry [13], [14], [25], [27], [54].

When symmetry is distorted by perspectivity, the detection of the underlying symmetry becomes non-trivial, thus complicating symmetry aided segmentation. In this case, even a perfectly symmetrical image is not identical to its symmetrical counterpart. We approach this difficulty by performing registration between the symmetrical counterparts. The registration process is justified by showing that an image of a symmetrical object, distorted by a projective transformation, relates to its symmetrical counterpart by a planar projective homography. A key result presented in this manuscript is the structure of this homography, which is determined, up to well defined limits, by the distorting projective transformation. A significant gain from this result is the waiving of the potentially obstructive phase of symmetry axis detection - an essential step in most previous symmetry oriented frameworks.

Figs. 2-3 illustrate the main idea of the proposed framework. Fig. 2a shows an approximately symmetrical object (its upper-left part is corrupted) that underwent a perspective distortion. Fig. 2b is a reflection of Fig. 2a with respect to the vertical symmetry axis of the image domain. Note however that this is not the symmetry axis of the object, which is unknown. We call Fig. 2b the *symmetrical counterpart* of Fig. 2a. Fig. 2a-b can be considered as two views of

the same object. Fig. 2b can be aligned to Fig. 2a by applying a perspective transformation different from the counter reflection, as shown in Fig. 2c. Superposition of Fig. 2a and Fig. 2c yields the complete non-corrupted object view as shown in Fig. 2d. In the course of the iterative segmentation process the symmetrical counterpart of the object delineated provides a dynamic shape prior² and thus facilitates the recovery of the hidden or vague object boundaries.

Fig. 3 demonstrates the detection of symmetrical objects. In Fig. 3a only one of the flowers imaged has rotational symmetry (up to an affine transformation). The symmetrical counterpart image (Fig. 3b) is generated by rotation of the image domain. Fig. 3c shows the superposition of the images displayed in Fig. 3a,b. Fig. 3d presents the superposition of the original image (Fig. 3a) and its symmetrical counterpart aligned to it. Note that the alignment between the two images was not obtained by the counter rotation but by an affine transformation.

The paper contains two fundamental, related contributions. The first is the use of an intrinsic shape property - symmetry - as a prior for image segmentation. This is made possible by a group of theoretical results related to symmetry and perspectivity which are the essence of the second contribution. Specifically we present the structure of the homography that relates an image (or a level-set function) to its symmetrical counterpart. The unknown projective transformation that distorts the object symmetry can be recovered from this homography under certain conditions. These conditions are specified, defining the concept of *symmetry preserving transformation*. We show that the transformation applied to a symmetrical image (or a labeling function) cannot be recovered from the homography that aligns symmetrical counterparts if it does not distort the image (or labeling function) symmetry. We propose a measure for the ‘distance’ between a labeling function and its aligned symmetrical counterpart. We call it the *symmetry imperfection measure*. This measure is the basis of the symmetry constraint that is incorporated within a unified segmentation functional. The suggested segmentation method is demonstrated on various images of approximately symmetrical objects distorted by planar projective transformation.

The paper is organized as follows. In section II we review the level-set formulation, showing its use for dynamic shape representation and segmentation. In section III the concepts of symmetry and projectivity are reviewed. The main theoretical contribution resides in subsection III-C which

²The word ‘dynamic’ in the expression ‘dynamic shape prior’ relates to the evolution of the level-set function (and its symmetrical counterpart) at each iteration. The same expression was introduced in a different context in [6], [24] to denote shape prior which captures the temporal evolution of shape.

establishes the key elements of the suggested study. In particular, the structure of the homography that relates between symmetrical counterpart images is analyzed. In section IV, a measure of *symmetry imperfection* of *approximately symmetrical* images, based on that homography, is defined. We use this measure to construct a symmetry-shape term. Implementation details and further implications are presented in section V. Experimental results are provided in section VI. We conclude in section VII.

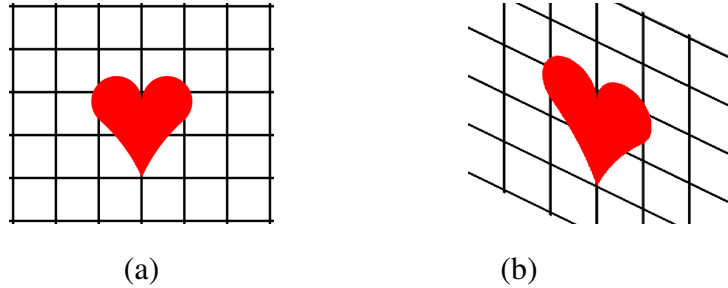


Fig. 1. *Shape transformation*. The coordinate transformation applied to the domain of the object indicator function transforms the represented shape accordingly.

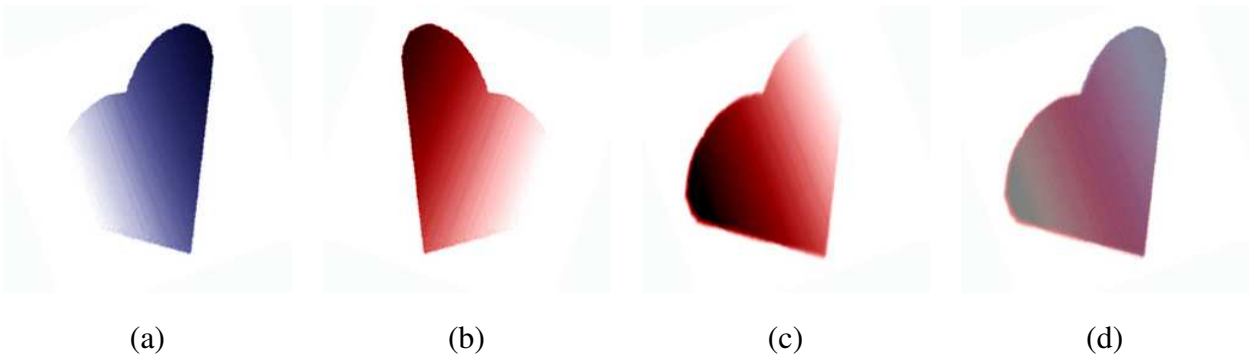


Fig. 2. (a) Image of approximately symmetrical object distorted by perspective. (b) The *symmetrical counterpart* of (a) is the reflection of (a) along the vertical symmetry axis of the image domain. (c) The image (b) aligned to (a) by a planar projective transformation. (d) Superposition of the image (a) with the image (c). The corrupted shape is recovered.

II. LEVEL-SETS FRAMEWORK

We use the level-set formulation [11], [33] since it allows non-parametric representation of the evolving object boundary and automatic changes of its topology. These characteristics are

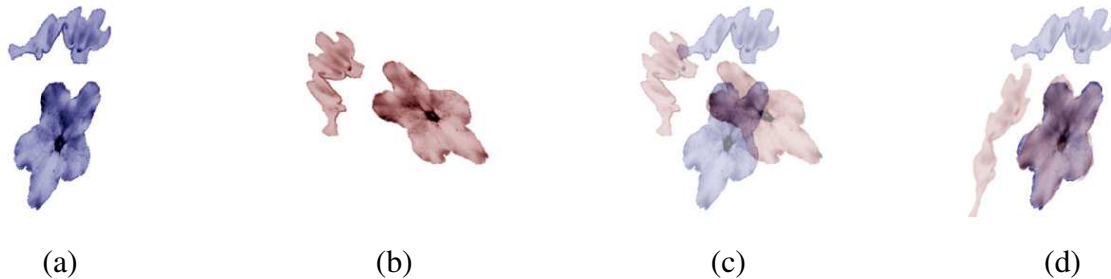


Fig. 3. (a) The image contains an object with rotational symmetry distorted by affine transformation. (b) The *symmetrical counterpart* of (a) – Rotation of the image plane (a) by 90° . (c) Superposition of (a) and (b). (d) Superposition of the image (a) with the image (b) aligned to (a) by an affine transformation. The object with rotational symmetry can be extracted.

also most desirable for the dynamic representation of the shape of the image region bounded by the zero level - an essential element of the proposed method.

A. Level-set formulation

Let I denote an image defined on the domain $\Omega \subset \mathbb{R}^2$. We define a closed contour $C \in \Omega$, that partitions the image domain Ω into two disjoint open subsets: ω and $\Omega \setminus \omega$. Without loss of generality, the image pixels $\{(x, y) = \mathbf{x} \mid \mathbf{x} \in \omega\}$ will be attributed to the object domain. Using the level-set framework [33] we define the evolving curve $C(t)$ as the zero level of a level-set function $\phi: \Omega \rightarrow \mathbb{R}$ at time t :

$$C(t) = \{\mathbf{x} \in \Omega \mid \phi(\mathbf{x}, t) = 0\}. \quad (1)$$

The optimal segmentation is therefore inferred by minimizing a cost functional $E(\phi, I)$ with respect to ϕ . The optimizer ϕ is derived iteratively by $\phi(t + \Delta t) = \phi(t) + \phi_t \Delta t$. The gradient descent equation ϕ_t is obtained from the first variation of the segmentation functional using the Euler-Lagrange equations.

The suggested segmentation framework utilizes a unified functional which consists of an energy term driven by the symmetry constraint together with the classical terms derived from the constraints related to the low-level image features.

$$E(\phi, I) = E_{\text{DATA}}(\phi, I) + E_{\text{SYM}}(\phi) \quad (2)$$

The data terms of E_{DATA} are briefly reviewed in subsections II-B, II-C and II-D based on current state-of-the-art level-set segmentation methods [3], [2], [20], [22], [51]. Subsection II-E outlines

the main idea behind the prior shape constraint [38] which is the ‘predecessor’ of the shape-symmetry term. The remainder of the paper relates to E_{SYM} .

B. Region-based term

In the spirit of the Mumford-Shah observation [32], we assume that the object contour $C = \partial\omega$, represented by zero level of ϕ , delimits homogeneous image regions. We use the Heaviside function (as in [3]) to assign the positive levels of ϕ to the object domain (ω) and the negative levels to the background domain ($\Omega \setminus \omega$):

$$H(\phi(t)) = \begin{cases} 1 & \phi(t) \geq 0 \\ 0 & \text{otherwise} \end{cases} \quad (3)$$

Let $I_{\text{in}}: \omega \rightarrow \mathbb{R}^+$ and $I_{\text{out}}: \Omega \setminus \omega \rightarrow \mathbb{R}^+$ be the image foreground and background intensities, respectively. Denoting the gray levels averages by $\{u_1^+ = \bar{I}_{\text{in}}, u_1^- = \bar{I}_{\text{out}}\}$ and the respective gray level variances by $\{u_2^+, u_2^-\}$, we look for a level-set function ϕ that minimizes the following *region-based* (RB) term [3], [28], [52]:

$$E_{\text{RB}}(\phi) = \int_{\Omega} \sum_{i=1}^2 [(G_i^+(I(\mathbf{x})) - u_i^+)^2 H(\phi) + (G_i^-(I(\mathbf{x})) - u_i^-)^2 (1 - H(\phi))] d\mathbf{x}, \quad (4)$$

where $G_1^+(I) = G_1^-(I) = I$ and $G_2^+(I) = \overline{(I(\mathbf{x}) - \bar{I}_{\text{in}})^2}$ $G_2^-(I) = \overline{(I(\mathbf{x}) - \bar{I}_{\text{out}})^2}$.

The level-set function ϕ is updated by the gradient descent equation:

$$\phi_t^{RB} = \delta(\phi) \sum_{i=1}^2 [-(G_i^+(I(\mathbf{x})) - u_i^+)^2 + (G_i^-(I(\mathbf{x})) - u_i^-)^2]. \quad (5)$$

The sets of scalars $\{u_i^+\}$ and $\{u_i^-\}$ are updated alternately with the evaluation of $\phi(t)$:

$$\begin{aligned} u_i^+ &= A^+ \int_{\Omega} G_i^+(I(\mathbf{x})) H(\phi) d\mathbf{x} \\ u_i^- &= A^- \int_{\Omega} G_i^-(I(\mathbf{x})) (1 - H(\phi)) d\mathbf{x} \end{aligned} \quad (6)$$

where $A^+ = 1 / \int_{\Omega} H(\phi) d\mathbf{x}$ and $A^- = 1 / \int_{\Omega} (1 - H(\phi)) d\mathbf{x}$.

Practically, a smooth approximation of the Heaviside function rather than a step function is used [3]:

$$H_{\epsilon}(\phi) = \frac{1}{2} \left(1 + \frac{2}{\pi} \arctan\left(\frac{\phi}{\epsilon}\right) \right). \quad (7)$$

The evolution of ϕ at each time step is weighted by the derivative of the regularized form of the Heaviside function:

$$\delta_{\epsilon}(\phi) = \frac{dH(\phi)}{d\phi} = \frac{1}{\pi} \frac{\epsilon}{\epsilon^2 + \phi^2}.$$

To simplify the notation, the subscript ϵ will be hereafter omitted.

C. Geodesic active contour and smoothness terms

The edge based segmentation criterion is derived from the assumption that the object boundaries coincides with the local maxima of the absolute values of the image gradients. Let $\nabla I(x, y) = \{I_x, I_y\} = \left\{ \frac{\partial I(x,y)}{\partial x}, \frac{\partial I(x,y)}{\partial y} \right\}$ denote the vector field of the image gradients. Following [20], [2], the inverse edge indicator function g is defined by:

$$g(\nabla I(\mathbf{x})) = 1/(\gamma + |\nabla I(\mathbf{x})|^2), \quad (8)$$

where γ is a small and positive scalar. The *geodesic active contour* (GAC) energy term

$$E_{\text{GAC}} = \int_{\Omega} g(\nabla I(\mathbf{x})) |\nabla H(\phi(\mathbf{x}))| d\mathbf{x}, \quad (9)$$

integrates the inverse edge indicator along the evolving contour. The evolution of ϕ is determined by:

$$\phi_t^{\text{GAC}} = \delta(\phi) \text{div} \left(g(\nabla I) \frac{\nabla \phi}{|\nabla \phi|} \right). \quad (10)$$

The GAC term reduces to the commonly used (e.g. [3]) smoothness term setting $g = 1$:

$$E_{\text{LEN}} = \int_{\Omega} |\nabla H(\phi(\mathbf{x}))| d\mathbf{x} \quad (11)$$

Minimizing (11) with respect to ϕ , we obtain the evolution equation:

$$\phi_t^{\text{LEN}} = \delta(\phi) \text{div} \left(\frac{\nabla \phi}{|\nabla \phi|} \right). \quad (12)$$

D. Edge alignment term

The *edge alignment* term (EA) constrains the level-set normal direction $\vec{n} = \frac{\nabla \phi}{|\nabla \phi|}$ to align with the image gradient direction ∇I [51], [21], [22]:

$$E_{\text{EA}} = - \int_{\Omega} \left| \left\langle \nabla I, \frac{\nabla \phi}{|\nabla \phi|} \right\rangle \right| |\nabla H(\phi)| d\mathbf{x}. \quad (13)$$

The associated gradient descent equation is:

$$\phi_t^{\text{EA}} = -\delta(\phi) \text{sign}(\langle \nabla \phi, \nabla I \rangle) \Delta I, \quad (14)$$

where $\langle \cdot, \cdot \rangle$ denotes the inner-product operation.

E. From shape constraint to shape symmetry constraint

Shape constraint, in level-set based segmentation techniques, is commonly defined by a dissimilarity measure between the evolving level-set function and a representation of the prior shape [4], [7], [10], [8], [9], [26], [38], [41], [47]. The main difficulty stems from the fact that the prior shape and the shape to segment are not aligned. Hence, shape transformations must be taken into consideration and the segmentation should be accompanied by a registration process.

1) *Shape transformations*: Transformation of the shape defined by the propagating contour is obtained by a coordinate transformation of the image domain Ω [38]. Let \mathcal{H} denote a 3×3 matrix that represents a planar transformation³. The matrix \mathcal{H} operates on homogeneous vectors $\mathbf{X} = (\mathbf{x}, 1)^T = (x, y, 1)^T$. We define an operator $h: \Omega \rightarrow \tilde{\Omega}$, where $\tilde{\Omega} \in \mathbb{P}^2$ is the projective domain, such that $h(\mathbf{x}) = \mathbf{X}$. Let $\mathbf{X}' = (X', Y', b) = \mathcal{H}\mathbf{X}$ denote the coordinate transformation of the projective domain $\tilde{\Omega}$. The entries of the 2-vector $\mathbf{x}' \in \Omega$ are the ratios of the first two coordinates of \mathbf{X}' and the third one, i.e. $\mathbf{x}' = (x', y') = (X'/b, Y'/b)$. Equivalently one can use the ‘inverse’ operator $h^{-1}: \tilde{\Omega} \rightarrow \Omega$ and write $h^{-1}(\mathbf{X}') = \mathbf{x}'$.

Let $L(\mathbf{x}) = H(\phi(\mathbf{x}))$ denote the indicator function of the object currently being segmented. Transformation of $L(\mathbf{x})$ by a planar transformation \mathcal{H} will be denoted by $L \circ \mathcal{H} \equiv L(\mathcal{H}\mathbf{x})$, where $\mathcal{H}\mathbf{x}$ is a shorthand to $h^{-1}(\mathcal{H}(h(\mathbf{x})))$. Fig. 1 illustrates this notion. We can also use the coordinate transformation to define shape symmetry, for example, if $L(\mathbf{x}) = L(x, y)$ embeds a shape with left-right bilateral symmetry then $L(x, y) = L(-x, y)$.

In general, we can think of L as a function defined on \mathbb{R}^2 where Ω is the support of the image. This way the operation \mathcal{H} maps vectors in \mathbb{R}^2 to vectors in \mathbb{R}^2 and is well defined. Note that the shape of the support may be changed under the action of the operator/matrix \mathcal{H} .

2) *Shape dissimilarity measure*: Let \tilde{L} be a binary representation of the prior shape. The segmentation process is defined by the evolution of the object indicator function L . A shape constraint takes the form $D(L(\mathbf{x}), \tilde{L}(\mathcal{H}\mathbf{x})) < \epsilon$ where D is a dissimilarity measure between $L(\mathbf{x})$ and the aligned prior shape representation $\tilde{L}(\mathcal{H}\mathbf{x})$. The matrix \mathcal{H} represents that alignment and is recovered concurrently with the segmentation process.

When only a single image is given, such prior is not available. Nevertheless, if an object is known to be symmetrical, its replicative form, induced by the symmetry, can be used. Specifically,

³Note that \mathcal{H} denotes the transformation while H denotes the Heaviside function.

we treat the image and its symmetrical counterpart (e.g. its reflection or rotation) as if they are two different views of the same object. The instantaneous symmetrical counterpart of the evolving shape provides a dynamic shape prior. The symmetry dissimilarity measure is based on a theoretical framework established in section III. Section IV considers the incorporation of the symmetry constraint within a level-set framework for segmentation.

III. SYMMETRY AND PROJECTIVITY

A. Symmetry

Symmetry is an intrinsic property of an object. An object is symmetrical with respect to a given operation if it remains invariant under that operation. In $2D$ geometry these operations relate to the basic planar Euclidean isometries: reflection, rotation and translation. We denote the symmetry operator by S . The operator S is an isometry that operates on homogeneous vectors $\mathbf{X} = (\mathbf{x}, 1)^T = (x, y, 1)^T$ and is represented as

$$S = \begin{vmatrix} \mathbf{s}R(\theta) & \mathbf{t} \\ \mathbf{0}^T & 1 \end{vmatrix} \quad (15)$$

where \mathbf{t} is a $2D$ translation vector, $\mathbf{0}$ is the null $2D$ vector, R is a 2×2 rotation matrix and \mathbf{s} is the diagonal matrix $\text{diag}(\pm 1, \pm 1)$.

Specifically, we consider *either* of the following transformations:

- 1) S is translation if $\mathbf{t} \neq \mathbf{0}$ and $\mathbf{s} = R(\theta) = \text{diag}(1, 1)$.
- 2) S is rotation if $\mathbf{t} = \mathbf{0}$, $\mathbf{s} = \text{diag}(1, 1)$ and $\theta \neq 0$.
- 3) S is reflection if $\mathbf{t} = \mathbf{0}$, $\theta = 0$ and \mathbf{s} is either $\text{diag}(-1, 1)$ for left-right reflection or $\text{diag}(1, -1)$ for up-down reflection.

In the case of reflection, the symmetry operation *reverses orientation*, otherwise (translation and rotation) it is *orientation preserving*.

The particular case of translational symmetry requires an infinite image domain. Hence, it is not specifically considered in this manuscript.

Definition 1 (Symmetrical image): Let S denote a symmetry operator as defined in (15). The operator S is either reflection or rotation. The image $I: \Omega \rightarrow \mathbb{R}^+$ is symmetrical with respect to S if

$$I(\mathbf{x}) = I(S\mathbf{x}) \equiv I \circ S \quad (16)$$

The concept of symmetry is intimately related to the notion of invariance. We say that a vector or a function L is invariant with respect to the transformation (or operator) S if $SL = L$.

Since we are interested in symmetry in terms of shape and not in terms of gray levels, we will therefore consider the *object indicator function* $L: \Omega \rightarrow \{0, 1\}$ as defined in subsection II-E. Hereafter, we use the shorthand notation for the coordinate transformation of the image domain as defined in subsection II-E.

Definition 2 (Symmetrical counterpart): Let S denote a symmetry operator. The object indicator function $\hat{L}(\mathbf{x}) = L \circ S(\mathbf{x}) = L(S\mathbf{x})$ is the *symmetrical counterpart* of $L(\mathbf{x})$. L is symmetrical iff $L = \hat{L}$.

We claim that the object indicator function of a symmetrical object distorted by a projective transformation is related to its symmetrical counterpart by projective transformation different from the defining symmetry. Before we proceed proving this claim we recall the definition of projective transformation.

B. Projectivity

This subsection follows the definitions in [15].

Definition 3: A planar projective transformation (projectivity) is a linear transformation represented by a non-singular 3×3 matrix \mathcal{H} operating on homogeneous vectors, $\mathbf{X}' = \mathcal{H}\mathbf{X}$, where,

$$\mathcal{H} = \begin{bmatrix} h_{11} & h_{12} & h_{13} \\ h_{21} & h_{22} & h_{23} \\ h_{31} & h_{32} & h_{33} \end{bmatrix} \quad (17)$$

Important specializations of the group formed by projective transformation are the affine group and the similarity group which is a subgroup of the affine group. These groups form a hierarchy of transformations. A similarity transformation is represented by

$$\mathcal{H}_{\text{SIM}} = \begin{bmatrix} \kappa R(\theta) & \mathbf{t} \\ \mathbf{0}^T & 1 \end{bmatrix} \quad (18)$$

where R is a 2×2 rotation (by θ) matrix and κ is an isotropic scaling. When $\kappa = 1$, \mathcal{H}_{SIM} is the Euclidean transformation denoted by \mathcal{H}_E . An affine transformation is obtained by multiplying

the matrix \mathcal{H}_{SIM} with

$$\mathcal{H}_A = \begin{bmatrix} K & \mathbf{0} \\ \mathbf{0}^T & 1 \end{bmatrix}. \quad (19)$$

K is an upper-triangular matrix normalized as $\text{Det}K = 1$. The matrix \mathcal{H}_P defines the ‘essence’ [15] of the projective transformation and takes the form:

$$\mathcal{H}_P = \begin{bmatrix} \mathbf{1} & \mathbf{0} \\ \mathbf{v}^T & v \end{bmatrix}, \quad (20)$$

where $\mathbf{1}$ is the 2-identity matrix. A projective transformation can be decomposed into a chain of transformations of a descending (or ascending) hierarchy order,

$$\mathcal{H} = \mathcal{H}_{\text{SIM}}\mathcal{H}_A\mathcal{H}_P = \begin{bmatrix} \mathbf{A} & \mathbf{t} \\ \mathbf{v}^T & v \end{bmatrix} \quad (21)$$

where $v \neq 0$ and $\mathbf{A} = \kappa RK + \mathbf{t}\mathbf{v}^T$ is a non-singular matrix.

C. Theoretical Results

In this subsection we consider the relation between an image (or an object indicator function) of a symmetrical object distorted by planar projective transformation \mathcal{H} and its symmetrical counterpart. The object indicator function L will be treated as a binary image and will be called for simplicity - *image*.

Recall from the previous subsection that a symmetrical image (or labeling function) L with respect to the symmetry operator S is invariant to S . We next define an operator (matrix) $S_{\mathcal{H}}$ such that a symmetrical image that underwent a planar projective transformation is *invariant* to its operation.

Theorem 1: Let $L_{\mathcal{H}} = L(\mathcal{H}\mathbf{x})$ denote the image obtained from the symmetrical image L by applying a planar projective transformation \mathcal{H} . If L is invariant to S , i.e. $L(\mathbf{x}) = L(S\mathbf{x}) = L(S^{-1}\mathbf{x})$ then $L_{\mathcal{H}}$ is invariant to $S_{\mathcal{H}}$ where $S_{\mathcal{H}} = \mathcal{H}^{-1}S\mathcal{H} \equiv \mathcal{H}^{-1}S^{-1}\mathcal{H}$.

Proof: We need to prove that $L_{\mathcal{H}}(\mathbf{x}) = L_{\mathcal{H}}(S_{\mathcal{H}}\mathbf{x})$.

We define $\mathbf{y} = \mathcal{H}\mathbf{x}$.

$$\begin{aligned} L_{\mathcal{H}}(S_{\mathcal{H}}\mathbf{x}) &= L_{\mathcal{H}}(\mathcal{H}^{-1}S\mathcal{H}\mathbf{x}) = L(S\mathcal{H}\mathbf{x}) \\ &= L(S\mathbf{y}) = L(\mathbf{y}) \\ &= L(\mathcal{H}\mathbf{x}) = L_{\mathcal{H}}(\mathbf{x}) \end{aligned} \quad (22)$$

We now use the result obtained in Theorem 1 to define the structure of the homography that aligns symmetrical counterpart images. ■

Theorem 2: Let $L_{\mathcal{H}}$ denote the image obtained from the symmetrical image L by applying a planar projective transformation \mathcal{H} . Let $\hat{L}_{\mathcal{H}} = L_{\mathcal{H}}(S\mathbf{x}) \equiv L_{\mathcal{H}} \circ S$ denote the symmetrical counterpart of $L_{\mathcal{H}}$ with respect to a symmetry operation S . The image $L_{\mathcal{H}}$ can be obtained from its symmetrical counterpart $\hat{L}_{\mathcal{H}}$ by applying a transformation represented by a 3×3 matrix of the form:

$$M = S^{-1}\mathcal{H}^{-1}S\mathcal{H}. \quad (23)$$

Proof: We need to prove that $L_{\mathcal{H}}(\mathbf{x}) = \hat{L}_{\mathcal{H}}(M\mathbf{x})$, where $M = S^{-1}\mathcal{H}^{-1}S\mathcal{H}$.

The image $L_{\mathcal{H}}$ is invariant to $S_{\mathcal{H}}$ thus $L_{\mathcal{H}}(\mathbf{x}) = L_{\mathcal{H}}(S_{\mathcal{H}}\mathbf{x})$. By definition, $\hat{L}_{\mathcal{H}}(\mathbf{x}) = L_{\mathcal{H}}(S\mathbf{x})$.

From the above equations and Theorem 1, defining $\mathbf{y} = S^{-1}S_{\mathcal{H}}\mathbf{x}$, we get:

$$\begin{aligned} L_{\mathcal{H}}(\mathbf{x}) &= L_{\mathcal{H}}(S_{\mathcal{H}}\mathbf{x}) = L_{\mathcal{H}}(SS^{-1}S_{\mathcal{H}}\mathbf{x}) \\ &= L_{\mathcal{H}}(S\mathbf{y}) = \hat{L}_{\mathcal{H}}(\mathbf{y}) \\ &= \hat{L}_{\mathcal{H}}(S^{-1}S_{\mathcal{H}}\mathbf{x}) = \hat{L}_{\mathcal{H}}(S^{-1}\mathcal{H}^{-1}S\mathcal{H}\mathbf{x}) \\ &= \hat{L}_{\mathcal{H}}(M\mathbf{x}). \end{aligned} \quad (24)$$

The image $L_{\mathcal{H}}$ can be generated from its symmetrical counterpart $\hat{L}_{\mathcal{H}}$ either by applying the inverse of the symmetry operation S or by a projective transformation M which is different from S^{-1} .

Let M_{INV} denote a 3×3 non-singular matrix such that $M_{\text{INV}} = \mathcal{H}^{-1}S^{-1}\mathcal{H}S$. M_{INV} is a projective transformation since $\mathcal{H}M_{\text{INV}} = S^{-1}\mathcal{H}S$ is a projective transformation according to:

$$S^{-1}\mathcal{H}S = S^{-1} \begin{bmatrix} \mathbf{A} & \mathbf{t} \\ \mathbf{v}^T & 1 \end{bmatrix} S = \begin{bmatrix} \mathbf{A}' & \mathbf{t}' \\ \mathbf{v}'^T & v' \end{bmatrix} = \mathcal{H}' \quad (25)$$

where \mathcal{H} is scaled such that $v = 1$.

Thus, $M = M_{\text{INV}}^{-1}$ represents a projective transformation. It is easy to prove that $M \neq S^{-1}$, when S is not the identity matrix. Assume to the contrary that there exists a non-singular \mathcal{H} and a symmetry operation S such that $M = S^{-1}$. Then, from (23), $S^{-1} = S^{-1}\mathcal{H}^{-1}S\mathcal{H}$. Thus, $\mathcal{H} = S\mathcal{H}$, which implies that either S is the identity matrix or \mathcal{H} is singular, in contradiction to the assumptions. ■

The next theorem gives tighter characterization of M .

Theorem 3: Let $L_{\mathcal{H}}$ denote the image obtained from the symmetrical image L by applying transformation \mathcal{H} . Let M denote the matrix that relates $L_{\mathcal{H}}$ to its symmetrical counterpart $\hat{L}_{\mathcal{H}}$. The matrices M and \mathcal{H} belong to the same subgroup of transformations (either projective or affine or similarity transformation).

The proof to this theorem appears in the Appendix.

Next, we argue that \mathcal{H} cannot be explicitly and fully recovered from M and S , if the operation of \mathcal{H} (or one of its factors) on a symmetrical image does not distort its symmetry.

Definition 4 (symmetry preserving transformation): Let L be a symmetrical image with respect to S . The projective transformation matrix \mathcal{H} is *symmetry preserving* if

$$L_{\mathcal{H}} = L(\mathcal{H}\mathbf{x}) = L(S\mathcal{H}\mathbf{x}) \quad (26)$$

Lemma 1: Let \mathcal{H} denote a symmetry preserving transformation with respect to the symmetry operation S . Then \mathcal{H} and S commute, i.e. $S\mathcal{H} = \mathcal{H}S$.

Proof: L is symmetrical, i.e. $L(\mathbf{x}) = L(S\mathbf{x})$. Applying the transformation \mathcal{H} on L we obtain: $L(\mathcal{H}\mathbf{x}) = L(\mathcal{H}S\mathbf{x})$. Since \mathcal{H} is symmetry preserving, $L(\mathcal{H}\mathbf{x})$ is symmetrical, thus $L(\mathcal{H}\mathbf{x}) = L(S\mathcal{H}\mathbf{x})$. The latter two equations prove the claim. ■

Theorem 4: Consider the image $L_{\mathcal{H}} = L(\mathcal{H}\mathbf{x})$, where L is a symmetrical image. Let $\hat{L}_{\mathcal{H}} = L(S\mathcal{H}\mathbf{x})$ denote its symmetrical counterpart. Let the matrix M satisfy Eq. (23), where $\hat{L}_{\mathcal{H}}(M\mathbf{x}) = L_{\mathcal{H}}(\mathbf{x})$. If \mathcal{H} can be factorized such that $\mathcal{H} = \mathcal{H}_S\tilde{\mathcal{H}}$ and \mathcal{H}_S denotes a symmetry preserving transformation with respect to S , then \mathcal{H} cannot be recovered from M .

Proof:

$$\begin{aligned} M &= S^{-1}\mathcal{H}^{-1}S\mathcal{H} \\ &= S^{-1}(\mathcal{H}_S\tilde{\mathcal{H}})^{-1}S\mathcal{H}_S\tilde{\mathcal{H}} = S^{-1}\tilde{\mathcal{H}}^{-1}\mathcal{H}_S^{-1}S\mathcal{H}_S\tilde{\mathcal{H}} \\ &= S^{-1}\tilde{\mathcal{H}}^{-1}\mathcal{H}_S^{-1}\mathcal{H}_S S\tilde{\mathcal{H}} \quad \text{since } S \text{ and } \mathcal{H}_S \text{ commute} \\ &= S^{-1}\tilde{\mathcal{H}}^{-1}S\tilde{\mathcal{H}} \end{aligned} \quad (27)$$

■

D. Examples

The claims made in Theorems 1-4 are exemplified for three particular cases. Consider, first, the image of the symmetrical object and its left-right reflection shown in Fig. 4a-b. Suppose that the image symmetry has been distorted by an Euclidean transformation of the form:

$$\mathcal{H}_E = \begin{bmatrix} \cos \theta & -\sin \theta & t_x \\ \sin \theta & \cos \theta & t_y \\ 0 & 0 & 1 \end{bmatrix}$$

Note that the Euclidean transformation is an isometry and thus preserves the object symmetry. However, it draws the symmetry axis of the object away from the symmetry axis of the image, rotating it by angle θ and translating it by t_x . Fig. 4a relates to its symmetrical counterpart by:

$$M = S^{-1}\mathcal{H}_E^{-1}S\mathcal{H}_E = \begin{bmatrix} \cos 2\theta & -\sin 2\theta & 2t_x \cos \theta \\ \sin 2\theta & \cos 2\theta & 2t_x \sin \theta \\ 0 & 0 & 1 \end{bmatrix},$$

where $S = (-1, 1, 1)$. Fig. 4a can thus be obtained from Fig. 4b by a rotation with angle 2θ and translation by $2R(\theta)[t_x, 0]^T$. Note that any translation parallel to the symmetry axis (in this case t_y) cannot be recovered from M . This expression for M implies that in the case of pure Euclidean transformation, the orientation of the object's symmetry axis can be recovered from M . Obviously M is an Euclidean transformation.

Consider, next the images shown in Fig. 4c-d. The object is distorted by a projective transformation \mathcal{H}_P :

$$\mathcal{H}_P = \begin{bmatrix} 1 & 0 & 0 \\ 0 & 1 & 0 \\ v_1 & v_2 & 1 \end{bmatrix}$$

The relation between the two images can be described by:

$$M = S^{-1}\mathcal{H}_P^{-1}S\mathcal{H}_P = \begin{bmatrix} 1 & 0 & 0 \\ 0 & 1 & 0 \\ 2v_1 & 0 & 1 \end{bmatrix}$$

When $v_2 \neq 0$ the object shape is distorted but its symmetry is preserved, thus v_2 cannot be recovered from M .

Finally, consider the object shown in Fig. 5. The object's appearance is invariant to rotation by

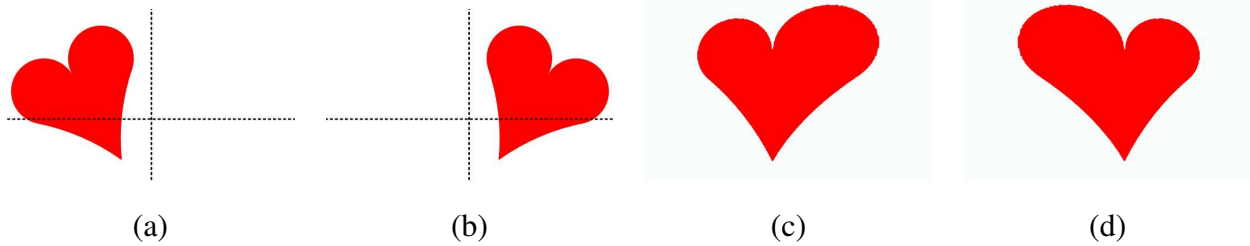


Fig. 4. (a) An image of a symmetrical object transformed by an Euclidean transformation: planar rotation by θ and then translation by \mathbf{t} . (b) The symmetrical counterpart of the image in (a). (c) An image of a symmetrical object distorted by projective transformation. (d) The symmetrical counterpart of the image in (c).

$n\pi/2$, where n is an integer. Let S denote rotation by $\pi/2$ i.e.

$$S = \begin{bmatrix} 0 & -1 & 0 \\ 1 & 0 & 0 \\ 0 & 0 & 1 \end{bmatrix}.$$

Fig. 5b is obtained by applying the affine transformation $\mathcal{H} = \mathcal{H}_{\text{SIM}}\mathcal{H}_A$ on Fig. 5a. Specifically, in this example

$$\mathcal{H} = \begin{bmatrix} R(\theta) & \mathbf{0} \\ \mathbf{0}^T & 1 \end{bmatrix} \begin{bmatrix} K & \mathbf{0} \\ \mathbf{0}^T & 1 \end{bmatrix}, \quad K = \begin{bmatrix} k_1 & k_2 \\ 0 & 1/k_1 \end{bmatrix}.$$

The scalars k_1 and k_2 determine the non-isotropic scaling: ratio and orientation. Fig. 5c is the symmetrical counterpart of Fig. 5b. It can be also obtained by applying M^{-1} on Fig. 5b, where M is of the form:

$$M = \begin{bmatrix} k_1^2 & k_1k_2 & 0 \\ k_1k_2 & 1/k_1^2 + k_2^2 & 0 \\ 0 & 0 & 1 \end{bmatrix}$$

Note, that the rotation θ has no effect on M .

IV. SYMMETRY BASED SEGMENTATION

A. Symmetry imperfection

In the current subsection we formalize the concept of *approximately symmetrical* shape. Specifically, two alternative definitions for ϵ -*symmetrical* images and *symmetry imperfection* measure are suggested. A symmetry imperfection measure indicates how ‘far’ the object is from

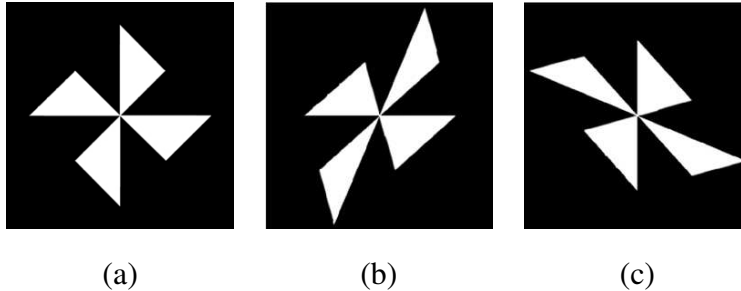


Fig. 5. (a) Schematic draw of a vane. The vane is symmetrical under rotation by $n\pi/4$, where n is an integer. (b) The vane (as in (a)) distorted by affine transformation. (c) The symmetrical counterpart of (b). This image can be generated from (b) either by clockwise rotation by 90° or by applying a projective transformation which captures the affine distortion of the vane.

being perfectly symmetrical. Shape symmetry is constrained by minimizing this measure. When symmetry is distorted by projectivity, defining a measure of symmetry imperfection is not trivial. We approach this difficulty relying on the results presented in Theorems 1,2.

Recall that a symmetrical binary image distorted by projective transformation is invariant to the operator $S_{\mathcal{H}}$ as defined in equation (22). This is the basis of the first definition.

Definition 5 (ϵ -symmetrical image; Symmetry imperfection (1)): The image L^ϵ is ϵ -symmetrical with respect to the symmetry operator S if $D(L^\epsilon, L^\epsilon \circ S) \leq \epsilon$, where D is a dissimilarity measure (distance function) and ϵ is a small and positive scalar. The measure $D(L^\epsilon, L^\epsilon \circ S)$ quantifies the *symmetry imperfection* of L^ϵ . Let $L_{\mathcal{H}}^\epsilon$ denote the image obtained from L^ϵ by applying a planar projective transformation \mathcal{H} . The measure for the symmetry imperfection of the *perspectively distorted* image $L_{\mathcal{H}}^\epsilon$ is defined by $D(L_{\mathcal{H}}^\epsilon, L_{\mathcal{H}}^\epsilon \circ S_{\mathcal{H}})$, where $S_{\mathcal{H}} = \mathcal{H}^{-1}S\mathcal{H}$.

Although this definition is natural, it is not always applicable, since usually the projective transformation \mathcal{H} is unknown. We therefore use an alternative equivalent definition of symmetry imperfection. This alternative measure involves the concept of the symmetrical counterpart image (see definition 2) and the homography M that aligns symmetrical counterpart images.

Definition 6 (Symmetry imperfection (2)): Let $L_{\mathcal{H}}^\epsilon$ be ϵ -symmetrical image distorted by planar projective homography \mathcal{H} . Let $\hat{L}_{\mathcal{H}}^\epsilon = L_{\mathcal{H}}^\epsilon \circ S$ denote the symmetrical counterpart of $L_{\mathcal{H}}^\epsilon$. The distance function $D(L_{\mathcal{H}}^\epsilon, \hat{L}_{\mathcal{H}}^\epsilon \circ M)$ measures the symmetry imperfection of $L_{\mathcal{H}}^\epsilon$.

Lemma 2: The two definitions are equivalent

Proof: Direct consequence of the identity $\hat{L}_{\mathcal{H}}^\epsilon \circ M = L_{\mathcal{H}}^\epsilon \circ S_{\mathcal{H}}$ ■

In the following subsections we show how M can be recovered during the segmentation process

by minimizing the term $\mathcal{D}_{\mathcal{H}} = D(L_{\mathcal{H}}^{\epsilon}, \hat{L}_{\mathcal{H}}^{\epsilon} \circ M)$ with respect to M . The recovery of M is easier when \mathcal{H} is either Euclidean or affine transformation, following the result of Theorem 3. In that case only 4 or 6 entries of M should be recovered. The matrix \mathcal{H} can be recovered from M up to a symmetry preserving transformation (Theorem 4).

B. Symmetry constraint

In the previous section the symmetrical counterparts were either images or object indicator functions. Using the level-set formulation, we will now refer to level-sets and their Heaviside functions, $H(\phi)$. Recall that $H(\phi(t))$ is an indicator function of the estimated object regions in the image at time t .

Let $\hat{\phi}: \Omega \rightarrow \mathbb{R}$ denote the symmetrical counterpart of ϕ with respect to a symmetry operation S . Specifically, $\hat{\phi}(\mathbf{x}) = \phi(S\mathbf{x})$ where S is either a reflection or a rotation matrix. We assume for now that S is known. This assumption will be relaxed in subsection V-F. Note however that \mathcal{H} is *unknown*. Let M denote the planar projective transformation that aligns $H(\hat{\phi})$ to $H(\phi)$ i.e. $H(\hat{\phi}) \circ M = H(\hat{\phi}(M\mathbf{x})) = H(\hat{\phi}_M)$. The matrix M is recovered by a registration process held concurrently with the segmentation, detailed in subsection IV-D.

Let $\mathcal{D} = D(H(\phi), H(\hat{\phi}_M))$ denote a dissimilarity measure between the evolving shape representation and its symmetrical counterpart. Note that if M is correctly recovered and ϕ captures a perfectly symmetrical object (up to projectivity) then \mathcal{D} should be zero. As shown in the previous subsection, \mathcal{D} is a measure for symmetry imperfection and therefore defines a shape symmetry constraint. The next subsection considers possible definitions of \mathcal{D} .

C. Biased shape dissimilarity measure

Consider, for example, the approximately symmetrical (up to projectivity) images shown in Fig. 6a,d. The object's symmetry is distorted by either deficiencies or excess parts. A straightforward definition of a symmetry shape constraint which measures the distance between the evolving segmentation and the aligned symmetrical counterpart takes the form:

$$D(\phi, \hat{\phi} | M) = \int_{\Omega} \left[H(\phi(\mathbf{x})) - H(\hat{\phi}_M) \right]^2 d\mathbf{x}. \quad (28)$$

However, incorporating this the unbiased shape constraint in the cost functional for segmentation, results in the *undesired* segmentation shown in Fig. 6b,e. This is due to the fact that the evolving

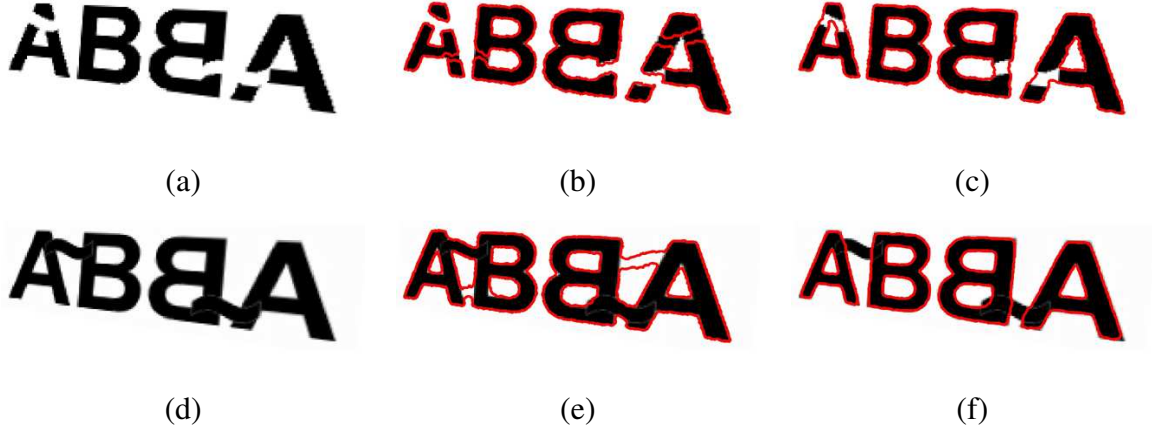


Fig. 6. (a, d) Images of symmetrical objects up to a projective transformation. The objects are distorted either by deficiencies (a) or by excess parts (d). (b, e) Segmentation (red) of the images in (a) and (d) respectively, using an *unbiased* dissimilarity measure between ϕ and its transformed reflection as in Eq. (28). Object segmentation is further spoiled due to the imperfection in its reflection. (c, f) Successful segmentation (red) using the *biased* dissimilarity measure as in Eq. (30).

level-set function ϕ is as imperfect as its symmetrical counterpart $\hat{\phi}$. To support a correct evolution of ϕ by $\hat{\phi}$, one has to account for the cause of the imperfection.

Refer again to Eq. (28). This dissimilarity measure integrates the non-overlapping object-background regions in both images indicated by $H(\phi)$ and $H(\hat{\phi})$. This is equivalent to a pointwise exclusive-or (xor) operation integrated over the image domain. We may thus rewrite the functional as follows:

$$D(\phi, \hat{\phi} | M) = \int_{\Omega} \left[H(\phi) \left(1 - H(\hat{\phi}_M) \right) + (1 - H(\phi)) H(\hat{\phi}_M) \right] dx \quad (29)$$

Note that the expressions (28) and (29) are identical, since $H(\phi) = (H(\phi))^2$. There are two types of ‘disagreement’ between the labeling of $H(\phi)$ and $H(\hat{\phi}_M)$. The first additive term in the right hand side of (29) is not zero for image regions labeled as *object* by ϕ and labeled as *background* by its symmetrical counterpart $\hat{\phi}$. The second additive term of (29) is not zero for image regions labeled as *background* by ϕ and labeled as *object* by $\hat{\phi}$. We can change the relative contribution of each term by a relative weight parameter $\mu \neq 0$:

$$E_{\text{SYM}} = \int_{\Omega} \left[\mu H(\phi) \left(1 - H(\hat{\phi}_M) \right) + (1 - H(\phi)) H(\hat{\phi}_M) \right] dx \quad (30)$$

The associated gradient equation for ϕ is then:

$$\phi_t^{\text{SYM}} = \delta(\phi) [H(\hat{\phi}_M) - \mu(1 - H(\hat{\phi}_M))] \quad (31)$$

Now, if excess parts are assumed, the left penalty term should be dominant, setting $\mu > 1$. Otherwise, if deficiencies are assumed, the right penalty term should be dominant, setting $\mu < 1$. Fig. 6c,f show segmentation of symmetrical objects with either deficiencies or excess parts, incorporating the shape term (30) within the segmentation functional. We used $\mu = 0.8$ and $\mu = 2$ for the segmentation of Fig. 6c and Fig. 6f, respectively. A similar dissimilarity measure was proposed in [40], [39] to quantify the ‘distance’ between the alternately evolving level-set functions of two different object views.

D. Recovery of the transformation

In the previous subsection we defined a biased symmetry imperfection measure E_{SYM} (Eq. 30) that measures the mismatch between $H(\phi)$ and its aligned symmetrical counterpart $H(\hat{\phi}_M)$. We now look for the optimal alignment matrix M that minimizes E_{SYM} .

Using the notation defined in subsection II-E, we define the coordinate transformation \mathcal{M} of $\hat{\phi}(\mathbf{x})$ as follows:

$$\mathcal{M}H(\hat{\phi}(\mathbf{x})) = H(\hat{\phi}(\mathbf{x})) \circ M = H(\hat{\phi}(M\mathbf{x})) \equiv H(\hat{\phi}_M) \quad (32)$$

We assume that the matrix M is a planar projective homography, as defined in equation (17). The eight unknown ratios of its entries $\hat{m}_k = m_{ij}/h_{33}$, $\{i, j\} = \{1, 1\}, \{1, 2\}, \dots, \{3, 2\}$ are recovered through the segmentation process, alternately with the evolution of the level-set function ϕ . The equations for \hat{m}_k are obtained by minimizing (30) with respect to each.

$$\frac{\partial \hat{m}_k}{\partial t} = \int_{\Omega} \delta(\hat{\phi}_M) [(1 - H(\phi)) - \mu H(\phi)] \frac{\partial \mathcal{M}(\hat{\phi})}{\partial \hat{m}_k} d\mathbf{x} \quad (33)$$

where

$$\frac{\partial \mathcal{M}(\hat{\phi})}{\partial \hat{m}_k} = \frac{\partial \mathcal{M}(\hat{\phi})}{\partial x} \left(\frac{\partial x}{\partial x'} \frac{\partial x'}{\partial \hat{m}_k} + \frac{\partial x}{\partial y'} \frac{\partial y'}{\partial \hat{m}_k} \right) + \frac{\partial \mathcal{M}(\hat{\phi})}{\partial y} \left(\frac{\partial y}{\partial x'} \frac{\partial x'}{\partial \hat{m}_k} + \frac{\partial y}{\partial y'} \frac{\partial y'}{\partial \hat{m}_k} \right) \quad (34)$$

Refer to [38], [36], [35] for detailed derivation of (33).

E. Unified segmentation functional

Symmetry-based, edge-based, region-based and smoothness constraints can be integrated to establish a comprehensive cost functional for segmentation:

$$E(\phi) = W^{\text{RB}} E_{\text{RB}}(\phi) + W^{\text{LEN}} E_{\text{LEN}}(\phi) + W^{\text{GAC}} E_{\text{GAC}}(\phi) + W^{\text{EA}} E_{\text{EA}}(\phi) + W^{\text{SYM}} E_{\text{SYM}}(\phi), \quad (35)$$

with equations (4, 11, 9, 13, 30).

Note that the smoothness (length) term (Eq. 11) is included in the GAC term E_{GAC} (Eq. 9). This can be shown by splitting $g(|\nabla I|)$ (eq. 8) as follows: $g(|\nabla I(\mathbf{x})|) = \gamma/(\gamma + |\nabla I|^2) = 1 - |\nabla I|^2/(\gamma + |\nabla I|^2)$, where the γ in the numerator of the left-hand side of the equation can be absorbed in the weight of the GAC term (see also [39]). In practice we zero either W^{GAC} (for noisy images) or W^{LEN} . The associated gradient descent equations ϕ_t are derived using the first variation of the functional (35)

$$\phi_t = W^{\text{RB}} \check{\phi}_t^{\text{RB}} + W^{\text{LEN}} \check{\phi}_t^{\text{LEN}} + W^{\text{GAC}} \check{\phi}_t^{\text{GAC}} + W^{\text{EA}} \check{\phi}_t^{\text{EA}} + W^{\text{SYM}} \check{\phi}_t^{\text{SYM}}. \quad (36)$$

The terms $\check{\phi}_t^{\text{TERM}}$ are obtained by slight modification of the gradient descent terms ϕ_t^{TERM} determined by equations (5, 12, 10, 14, 31). This issue and the determination of the weights W^{TERM} for the different terms in Eq.(36) are discussed in subsection V-C.

Refinement of the segmentation results can be obtained for images with multiple channels, $I: \Omega \rightarrow \mathbb{R}^n$, e.g. color images. The region-based term ϕ_t^{RB} and the alignment term ϕ_t^{EA} are thus the sum of the contributions of each channel I_i . Multi-channel segmentation is particularly suitable when the object boundaries are apparent in some of the channels while the piecewise homogeneity is preserved in others. Figure 10 demonstrates segmentation of a color image.

V. IMPLEMENTATION AND FURTHER IMPLICATIONS

Segmentation is obtained by minimizing a cost functional that incorporates symmetry as well as region-based, edge-based and smoothness terms. The minimizing level-set function is evolved concurrently with the registration of its instantaneous symmetrical counterpart to it. The symmetrical counterpart is generated by a flip or rotation of the coordinate system of the propagating level-set function. The evolution of the level-set function is controlled by the constraints imposed by the data of the associated image and by the its aligned symmetrical counterpart. The planar projective transformation between the evolving level-set function and its symmetrical counterpart is updated at each iteration.

A. Algorithm

We summarize the proposed algorithm for segmentation of a symmetric object distorted by projectivity.

- 1) Choose an initial level-set function $\phi_{t=0}$ that determines the initial segmentation contour.
- 2) Set initial values for the transformation parameters \hat{m}_k . For example, set M to the identity matrix.
- 3) Compute u_+ and u_- according to (6), based on the current contour interior and exterior, defined by $\phi(t)$.
- 4) Generate the symmetrical counterpart of $\phi(\mathbf{x})$, $\hat{\phi}(\mathbf{x}) = \phi(S\mathbf{x})$ when the symmetry operator S is known⁴.
- 5) Update the matrix M by recovering the transformation parameters m_k according to (33)
- 6) Update ϕ using the gradient descent equation (36).
- 7) Repeat steps 3-6 until convergence.

B. Initialization

The algorithm is quite robust to the selection of initial level-set function $\phi_0(\mathbf{x})$. The only limitation is that image regions labeled as foreground at the first iteration, i.e $\omega_0 = \{\mathbf{x} \mid \phi_0(\mathbf{x}) \geq 0\}$, should contain a significant portion of the object to be segmented, such that the calculated image features will approximately characterize the object region. Formally, we assume that $G^+(I(\omega_0)) \approx G^+(I(\hat{\omega}))$, where $\hat{\omega}$ is the actual object region in the image. When there exists an estimate of the average gray levels of either the foreground or the background image regions, this restriction can be eliminated.

We run the algorithm until the following stopping condition is met:

$$\sum_{\mathbf{x} \in \Omega} |H(\phi^{t+\Delta t}(\mathbf{x})) - H(\phi^t(\mathbf{x}))| < s$$

where s is a predefined threshold and $\phi^{t+\Delta t}(\mathbf{x})$ is the level-set function, at time $t + \Delta t$.

C. Setting the weights of the energy terms

When the solution to an image analysis problem is obtained by minimizing a cost functional, a ‘correct’ setting of the weights of the energy terms is of fundamental importance. Following our suggestion in [39], the weights of the terms in the functional presented in eq. (35) are adaptively set. The automatic and dynamic weight setting is carried out in two stages. First, we apply a

⁴When S is unknown, use $\hat{\phi}(\mathbf{x}) = \phi(T\mathbf{x})$ where T is of the same type as S . Refer to subsection V-F for further details.

thresholding operation to bound the dynamic range of $\phi_t(\mathbf{x})$. The threshold is determined by the standard deviation of $\phi_t(\mathbf{x})$ over Ω :

$$\check{\phi}_t^{\text{TERM}}(\mathbf{x}) = B(\phi_t^{\text{TERM}}(\mathbf{x})) = \begin{cases} U_B & \text{if } \phi_t^{\text{TERM}}(\mathbf{x}) > U_B \\ L_B & \text{if } \phi_t^{\text{TERM}}(\mathbf{x}) < L_B \\ \phi_t^{\text{TERM}}(\mathbf{x}) & \text{otherwise} \end{cases} \quad (37)$$

where

$$U_B = \text{std}(\phi_t^{\text{TERM}}(\mathbf{x})), \quad L_B = -U_B$$

Here, $\text{std}(\phi_t(\mathbf{x}))$ stands for the standard deviation of $\phi_t(\mathbf{x})$ over Ω . The functional $B(\cdot)$ operates on ϕ_t^{TERM} to bound its dynamic range. Next, the range of $|\check{\phi}_t^{\text{TERM}}|$ is normalized

$$W^{\text{TERM}} = 1 / \max_{\mathbf{x}} |\check{\phi}_t^{\text{TERM}}(\mathbf{x})|. \quad (38)$$

Note that the clipping (Eq. 37) affects only extreme values of ϕ_t^{TERM} , that is $\check{\phi}_t^{\text{TERM}}(\mathbf{x}) = \phi_t^{\text{TERM}}(\mathbf{x})$ for most $\mathbf{x} \in \Omega$. Since W is recalculated at each iteration it is time dependent. This formulation enables an automatic and adaptive determination of the weights of the energy terms.

D. Recovery of the transformation parameters

Minimizing the symmetry term (30) with respect to the eight unknown ratios of the homography matrix entries is a complicated computational task. As in [39], we perform a rough search in the 8 dimensional parameter space working on a coarse to fine set of grids before applying the gradient based Quasi-Newton method. The former search, done only *once*, significantly reduces the search space. The gradient based algorithm, applied in every iteration, refines the search result based on the updated level-set function.

It is worth noting that unlike other registration algorithms, obtaining a global minimum is undesired. This 'surprising' claim can be understood when observing that a global minimum of the registration process is obtained when $M = S^{-1}$, where S is the transformation used to generate the symmetrical counterpart. In this case the segmented object and its symmetrical counterpart would have a perfect match and the symmetry property is actually not used to facilitate the segmentation. To obtain a local minimum which is not a global one in the case of rotational symmetry we deliberately exclude the rotation that generates the symmetrical counterpart from the multi-grid one-time search performed prior to the steepest descent registration process. Note

that such global minima will not be obtained in the cases of bilateral symmetry since S is a reflecting transformation while the homography matrix M does not reverse orientation by definition [15].

Fig. 12c demonstrates the main point of the claim made above. The figure shows the evolving contour (red) together with the registered symmetrical counterpart (white) that was generated by a clockwise rotation of 90^0 . If the transformation parameters found by the registration process were equivalent to counterclockwise rotation by 90^0 the ‘defects’ in both the segmented wheel and the *registered* symmetrical counterpart would be located at the same place. Thus, the ‘missing parts’ could not be recovered.

E. Segmentation with multiple symmetrical counterparts

Consider the segmentation of an object with rotational symmetry. Let $\phi(t)$ denote its corresponding level-set function at time t and $L_{\mathcal{H}} = H(\phi(t))$ denote the respective object indicator function. If $L_{\mathcal{H}}$ is invariant to rotation by α degrees, where $\alpha \leq 2\pi/3$ then more than one symmetrical counterpart level-set functions can be used to support the segmentation. Specifically, the number of supportive symmetrical-counterpart level-set functions is $N = \lfloor 2\pi/\alpha \rfloor - 1$, since the object is invariant to rotations by $n\alpha^0$, where $n = 1 \dots N$. We denote this rotation by $R_{n\alpha}$. In that case, the symmetry constraint takes the following form:

$$E_{\text{SYM}} = \sum_{n=1}^N \int_{\Omega} \left[\mu H(\phi) \left(1 - H(\hat{\phi}_n \circ M_n) \right) + (1 - H(\phi)) H(\hat{\phi}_n \circ M_n) \right] d\mathbf{x}, \quad (39)$$

where, $\hat{\phi}_n = \phi(R_{n\alpha}\mathbf{x}) = \phi \circ R_{n\alpha}$ and M_n is the homography that aligns $\hat{\phi}_n$ to ϕ . The computational cost using this symmetry constraint is higher since N homographies M_n should be recovered. However, the eventual segmentation results are better, as shown in Fig. 13.

F. Segmentation when only the type of symmetry is known

In most practical applications S is not available. In this subsection we generalize the suggested framework assuming that only the type of symmetry (i.e. rotation or translation) is known. For example, we know that the object is rotationally symmetrical yet the precise rotation degree is not known. Alternatively the object is known to have a bilateral symmetry however we do not know if the bilateral symmetry is horizontal or vertical. Let $L = H(\phi)$ be invariant to the symmetry operator $S = R_{\alpha}$ where R_{α} is a planar clockwise rotation by α^0 . Let $L_{\mathcal{H}}$ be a

perspective distortion of L by \mathcal{H} . Consider the case where the symmetrical counterpart of $L_{\mathcal{H}}$ is generated by a planar clockwise rotation β^0 where $\beta \neq \alpha$, thus $\hat{L}_{\mathcal{H}}^{\beta} = L_{\mathcal{H}}(R_{\beta}\mathbf{x}) \equiv L_{\mathcal{H}} \circ R_{\beta}$. We define a *modified* symmetry imperfection measure of the following form: $D(L_{\mathcal{H}}, \hat{L}_{\mathcal{H}}^{\beta} \circ \tilde{M})$. The matrix \tilde{M} aligns $\hat{L}_{\mathcal{H}}^{\beta}$ to $L_{\mathcal{H}}$. The next theorem relates M and \tilde{M} .

Theorem 5: Let $L = L \circ S$ where $S = R_{\alpha}$. Let M be a planar projective homography such that $L_{\mathcal{H}}(\mathbf{x}) = \hat{L}_{\mathcal{H}}(M\mathbf{x})$ where $\hat{L}_{\mathcal{H}} = L_{\mathcal{H}}(R_{\alpha}\mathbf{x})$. We call $\hat{L}_{\mathcal{H}}$ the *standard* symmetrical counterpart. Suppose that $\hat{L}_{\mathcal{H}}^{\beta} = L_{\mathcal{H}}(R_{\beta}\mathbf{x})$ is generated from $L_{\mathcal{H}}$ by an arbitrary rotation β , where $\beta \neq \alpha$. We claim that $L_{\mathcal{H}} = \hat{L}_{\mathcal{H}}^{\beta}(\tilde{M}\mathbf{x})$, where $\tilde{M} = MR_{\alpha-\beta}$.

Proof: By definition, $\hat{L}_{\mathcal{H}}(\mathbf{x}) = L_{\mathcal{H}}(R_{\alpha}\mathbf{x})$ and $\hat{L}_{\mathcal{H}}^{\beta}(\mathbf{x}) = L_{\mathcal{H}}(R_{\beta}\mathbf{x})$. This implies that

$$\hat{L}_{\mathcal{H}}(\mathbf{x}) = \hat{L}_{\mathcal{H}}^{\beta}(R_{\alpha-\beta}\mathbf{x}) \quad (40)$$

Using Theorem 2 for the special case of $S = R_{\alpha}$ and the above definition of $\hat{L}_{\mathcal{H}}$, we get:

$$\hat{L}_{\mathcal{H}}(\mathbf{x}) = L_{\mathcal{H}}(M^{-1}\mathbf{x}). \quad (41)$$

From equations (40) and (41), we get: $L_{\mathcal{H}}(M^{-1}\mathbf{x}) = \hat{L}_{\mathcal{H}}^{\beta}(R_{\alpha-\beta}\mathbf{x})$. The latter equation implies that

$$L_{\mathcal{H}}(\mathbf{x}) = \hat{L}_{\mathcal{H}}^{\beta}(MR_{\alpha-\beta}\mathbf{x}) = \hat{L}_{\mathcal{H}}^{\beta}(\tilde{M}\mathbf{x}),$$

defining $\tilde{M} = MR_{\alpha-\beta}$.

The homography \tilde{M} is equivalent to M up to a rotation by $\alpha - \beta$ degrees. ■

Theorem 5 implies that when the symmetry operator is an unknown rotation, the symmetrical counterpart level-set function can be generated by an arbitrary rotation (e.g. $\pi/2$). In this case the recovered homography is equivalent to the homography of the *standard* symmetrical counterpart up to a planar rotation. The distorting projective transformation \mathcal{H} can be recovered up to a similarity transformation.

The result presented in Theorem 5 is also applicable to object with bilateral symmetry. An image (or any function defined on \mathbb{R}^2) reflected along its vertical axis can be aligned to its reflection along its horizontal axis by a rotation of $R = \pi$. Thus, $S_{\text{LR}} = R(\pi)S_{\text{UD}}$ where S_{LR} is an horizontal reflection and S_{UD} is a vertical reflection. Similarly, $S_{\text{UD}} = R(\pi)S_{\text{LR}}$.

VI. EXPERIMENTS

We demonstrate the proposed algorithm for the segmentation of approximately symmetrical objects in the presence of projective distortion. The images are displayed with the initial and

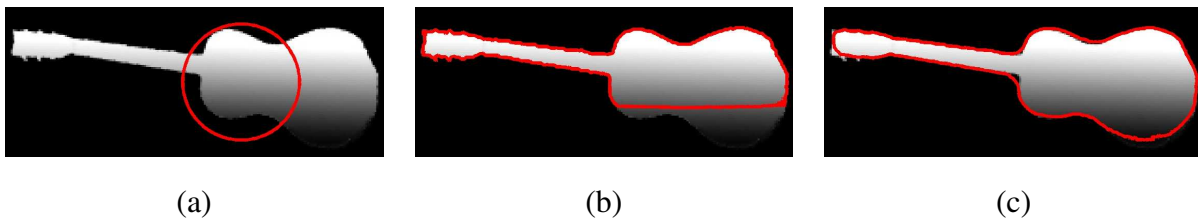


Fig. 7. (a) Input image of a symmetrical object with the initial segmentation contour (red). (b) Segmentation (red) without the symmetry constraint. (c) Successful segmentation (red) with the proposed algorithm.

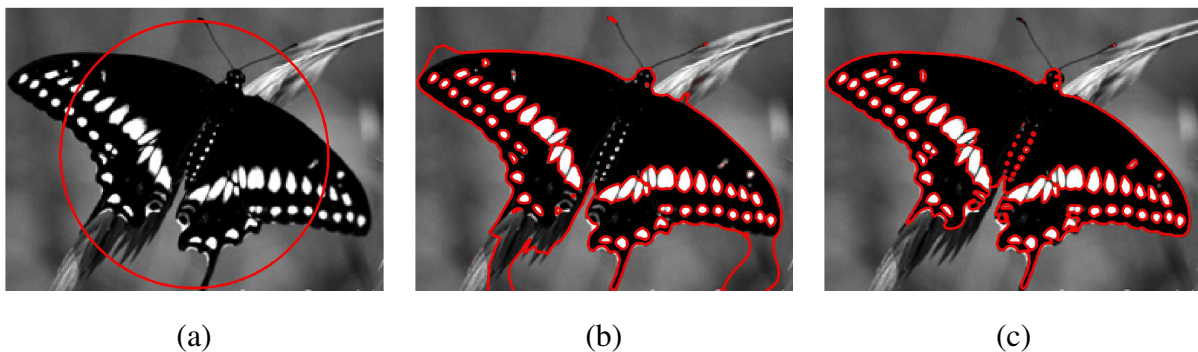


Fig. 8. (a) Input image of a symmetrical object with the initial segmentation contour (red). (b) Segmentation (red) without the symmetry constraint. (c) Successful segmentation (red) with the proposed algorithm. Original image courtesy of George Payne. URL: <http://cajunimages.com/images/butterfly%20wallpaper.jpg>

final segmenting contours. Segmentation results are compared to those obtained using the functional (35) without the symmetry term. The contribution of each term in the gradient descent equation (36) is bounded to $[-1, 1]$ as explained in subsection V-C. We used $\mu = 0.8$ for the segmentation of Figs. 7, 10, 12 assuming occlusions and $\mu = 2$ for the segmentation of Figs. 9, 8, 11, 13 where the symmetrical object has to be extracted from background image regions with the same gray levels. In Fig. 7 the upper part of the guitar is used to extract its lower part correctly. In the butterfly image shown in Fig. 8, a left-right reflection of the evolving level-set function is used to support accurate segmentation of the left wing of the butterfly. Since in this example the transformation \mathcal{H} is Euclidian, the orientation of the butterfly's symmetry axis can be easily recovered from M .

In Fig. 9 the approximately symmetrical object (man's shadow) is extracted based on the bilateral symmetry of the object. In this example, the initial level-set function ϕ_0 has been set to



Fig. 9. (a) Input image of a symmetrical object with the evolving segmentation contour (red) after one iteration. Here, ϕ_0 was set to zero while $u_0^+ = 0$ and $u_0^- = 1$. (b) Segmentation (red) without the symmetry constraint. (c) Successful segmentation (red) with the proposed algorithm. A video clip that demonstrates the contour evolution of this example is provided as supplemental material. Original image courtesy of Amit Jayant Deshpande. URL: <http://web.mit.edu/amitd/www/pics/chicago/shadow.jpg>

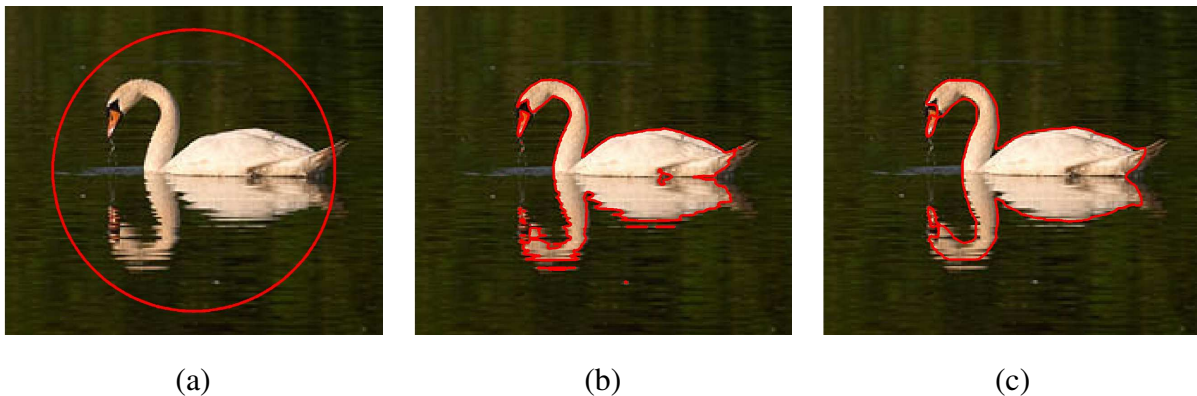


Fig. 10. (a) Input image of a symmetrical object with the initial segmentation contour (red). (b) Segmentation (red) without the symmetry constraint. (c) Successful segmentation (red) with the proposed algorithm. Original image courtesy of Richard Lindley. URL: <http://www.richardlindley.co.uk/links.htm>

an all-zero function - which implies no initial contour. Instead, the initial mean intensities have been set as follows: $u^+ = 0$; $u^- = 1$ assuming that the average intensity of the background is brighter than the foreground. We use this form of initialization to demonstrate the independence of the proposed algorithm with respect to the size, shape or orientation of the initial contour.



Fig. 11. (a) Input image of a symmetrical object with the evolving segmentation contour (red) after one iteration. Here, ϕ_0 was set to zero while $u_0^+ = 0$ and $u_0^- = 1$. (b) The vulture is extracted (red) although, based on the image intensities alone, it is inseparable from the tree. Original image courtesy of Allen Matheson URL: <http://thegreencuttingboard.blogspot.com/Vulture.jpg>

In the swan example shown in Fig. 10 we used both color and symmetry cues for correct extraction of the swan and its reflection. Based on the image intensities alone the vulture and the tree in Fig. 11 are inseparable. Adding the symmetry constraint the vulture is extracted as shown in Fig. 11b. In this example the segmentation is not precise because of the incorrect registration of the symmetrical counterpart to the evolving level-set function. The undesired local minimum obtained in the registration is probably due to the dominance of none-symmetric tree region.

The example shown in Fig. 12 demonstrates segmentation in the presence of rotational symmetry. The original image (not shown) is invariant to rotation by 60^0n , where $n = 1, 2 \dots 5$. Figs. 12a,e show the images to segment which are noisy, corrupted and transformed versions of the original image. Fig. 12b shows the symmetrical counterpart of the image in Fig. 12a obtained by a clockwise rotation of 90^0 . Practically, only the symmetrical counterpart of the evolving level-set function is used. The symmetrical counterpart image is shown here for demonstration. The segmenting contour (red) of the corrupted object in (a) is shown in Fig: 12c together with the *registered* symmetrical counterpart. Note that the symmetrical counterpart is *not* registered to the segmented object by a counterclockwise rotation of 90^0 but by a *different* transformation. Otherwise, there would have been a perfect match between the ‘defects’ in the image to segment and its registered symmetrical counterpart. The successful segmentations (red) of the image in Fig. 12a and Fig. 12e using the proposed symmetry-based algorithm is presented in Fig 12d and Fig. 12f respectively. Figs. 12g,h demonstrate unsuccessful segmentations (red) of the image

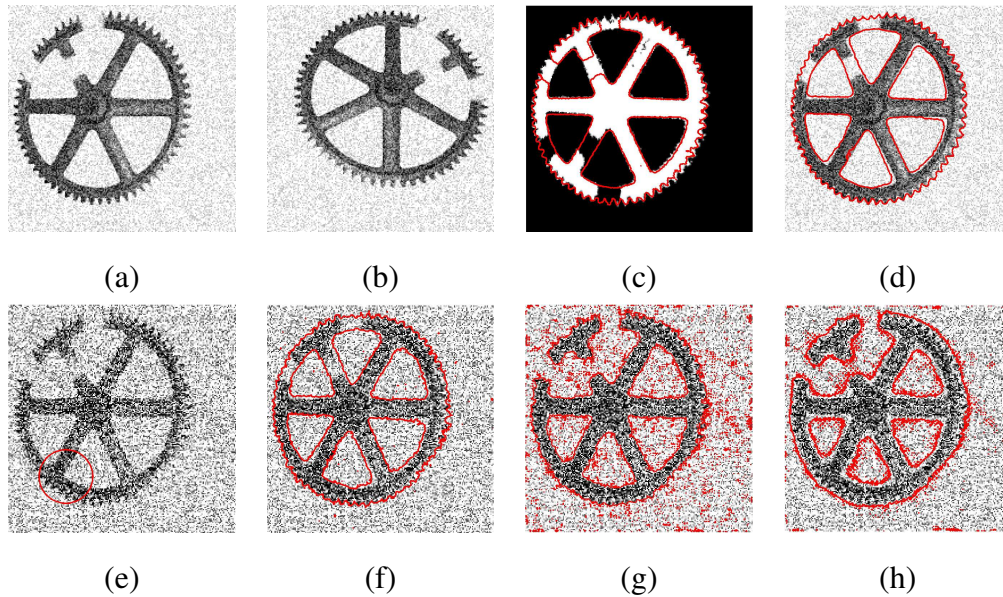


Fig. 12. (a) The image to segment. It is a noisy, corrupted and transformed version of an original image (not shown). The original image is invariant to rotation by $60^{\circ}n$, where $n = 1, 2 \dots 5$. (b) The symmetrical counterpart of the image in (a) obtained by a clockwise rotation of 90° . Practically, only the symmetrical counterpart of the evolving level-set function is used. The symmetrical counterpart image is shown here for demonstration. (c) The segmenting contour (red) of the object in (a) is shown together with the *registered* symmetrical counterpart. Note that the symmetrical counterpart is *not* registered to (a) by a counterclockwise rotation of 90° but by a *different* transformation. Otherwise, there would have been a perfect match between the ‘defects’ in the image to segment and its registered symmetrical counterpart. (d) Successful segmentation (red) of the image in (a) using the proposed symmetry-based algorithm. (e) Noisier version of the image in (a) together with the initial contour (red). (f) Successful segmentation (red) of the image in (e) using the proposed symmetry-based algorithm. (g, h) Unsuccessful segmentation (red) of the image in (e) using the Chan-Vese algorithm [3]. In (h) the contribution of the smoothness term was 4 times bigger than in (g).

in Fig. 12e using the Chan-Vese algorithm [3]. In Fig. 12h the contribution of the smoothness term was four times bigger than in Fig. 12g. Note that using the symmetrical counterpart we successfully overcome the noise.

In the last example, Fig. 13, segmentation of an object with approximate rotational symmetry is demonstrated. In this example we could theoretically use four symmetrical counterparts to support the segmentation. However as shown in Fig. 13d two symmetrical counterparts are sufficient. One of the symmetrical counterparts of the final level-set function is shown in Fig. 13f. We used the symmetry constraint for multiple symmetrical counterpart level-set functions according to equation (39).

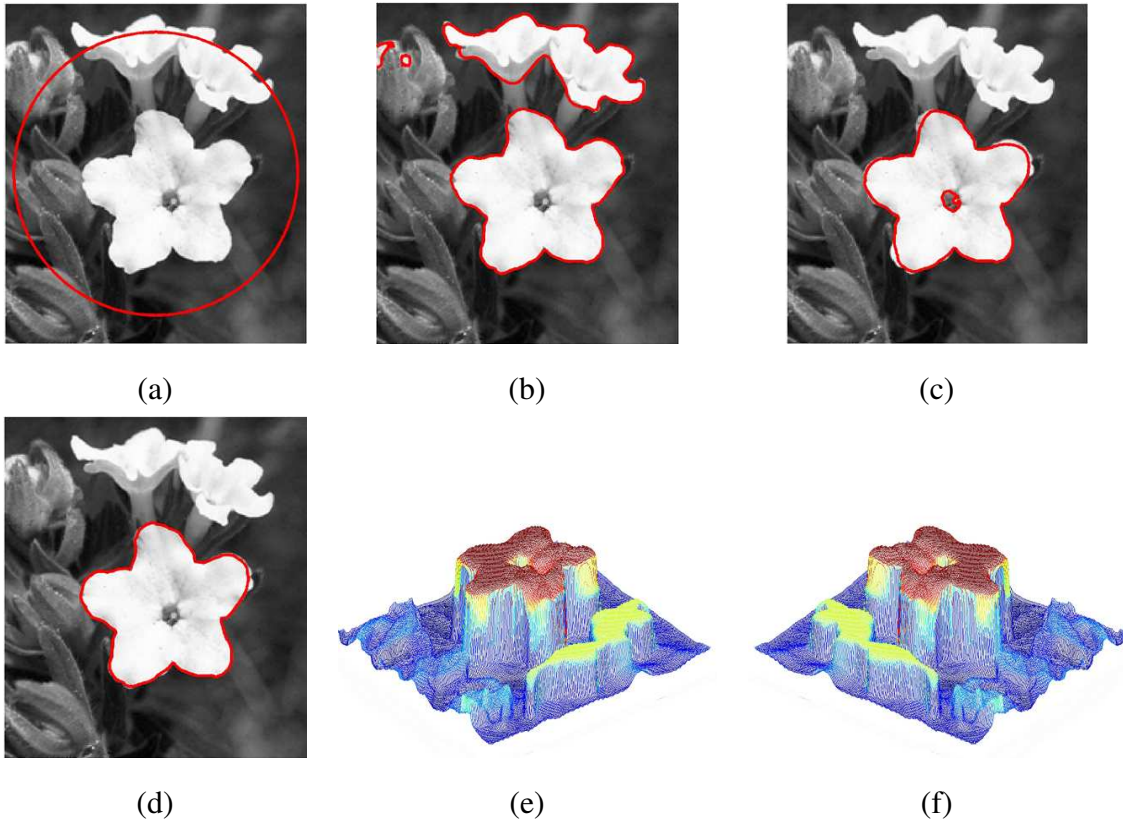


Fig. 13. (a) Input image rotationally symmetrical object. The object is invariant to rotation by $72^{\circ}n$ where $n = 1, 2, \dots, 4$. The initial segmentation contour (red) is shown. (b) Segmentation (red) without the symmetry constraint. (c) Segmentation (red) with the proposed algorithm using a single symmetrical counterpart. (d) Segmentation (red) with the proposed algorithm using two symmetrical counterparts. (e) Final level-set function. (f) One of the symmetrical counterparts of the level-set function (e), obtained by rotation by 90° . Original image courtesy of Kenneth R. Robertson. URL: <http://inhs.uiuc.edu>

VII. SUMMARY

The paper contains two fundamental, related contributions. The first is a variational framework for the segmentation of symmetrical objects distorted by perspective. The proposed segmentation method relies on theoretical results related to symmetry and perspective which are the essence of the second contribution.

Unlike most of the previous approaches to symmetry, the symmetrical object is considered as a single entity and not as a collection of landmarks or feature points. This is accomplished by using the level-set formulation and assigning, for example, the positive levels of the level-set function to the object domain and the negative levels to the background. An *object*, in the

proposed framework, is represented by the support of its respective labeling function. As the level-set function evolves, the corresponding labeling function and thus the represented object change accordingly.

A key concept in the suggested study is the symmetrical counterpart of the evolving level-set function, obtained by either rotation or reflection of the level-set function domain. We assume that the object to segment underwent a planar projective transformation, thus the source level-set function and its symmetrical counterpart are not identical. We show that these two level-set functions are related by planar projective homography.

Due to noise, occlusion, shadowing or assimilation with the background, the propagating object contour is only approximately symmetrical. We define a symmetry imperfection measure which is actually the ‘distance’ between the evolving level-set function and its aligned symmetrical counterpart. A symmetry constraint based on the symmetry imperfection measure is incorporated within the level-set based functional for segmentation. The homography matrix that aligns the symmetrical counterpart level-set functions is recovered concurrently with the segmentation.

We show in Theorem 2 that the recovered homography is determined by the projective transformation that distorts the image symmetry. This implies that the homography obtained by the alignment process of the symmetrical counterpart functions (or images) can be used for partial recovery of the 3D structure of the imaged symmetrical object. As implied from Theorem 4, full recovery is not possible if the projection of the 3D object on the image plane preserves its symmetry.

The algorithm suggested is demonstrated on various images of objects with either bilateral or rotational symmetry, distorted by projectivity. Promising segmentation results are shown. In this manuscript only shape symmetry is considered. The proposed framework can be extended considering symmetry in terms of gray levels or color. The notion of symmetrical counterpart can be thus applied to the image itself and not to binary (or level-set) functions. Possible applications are de-noising, super-resolution from a single symmetrical image and inpainting. All are subjects for future research.

APPENDIX A
PROOF OF THEOREM 3

Proof: The proof is divided into several sub-cases. When S is either rotation or translation, M is the product of Euclidean transformations (S, S^{-1}) and either Euclidean, similarity or affine transformations ($\mathcal{H}, \mathcal{H}^{-1}$). Thus M belongs to the respective subgroup of transformations. When $S = \text{diag}(s, 1)$ is reflection, i.e. s is either $(1, -1)$ or $(-1, 1)$ the claim can be simply proved by matrix multiplications. Specifically, when $\mathcal{H} = \mathcal{H}_{\text{SIM}}$ represents a similarity transformation, as defined in (18):

$$M = \begin{bmatrix} R(2\theta) & \mathbf{t}' \\ \mathbf{0}^T & 1 \end{bmatrix}, \quad \mathbf{t}' = \kappa^{-1} \mathbf{t}^T [\mathbf{1} - \text{diag}(s)] R(\theta)^T \quad (42)$$

When \mathcal{H} represents an affine transformation:

$$\mathcal{H} = \mathcal{H}_A = \begin{bmatrix} A & \mathbf{t} \\ \mathbf{0}^T & 1 \end{bmatrix}, \quad A = \begin{bmatrix} a_1 & a_2 \\ a_3 & a_4 \end{bmatrix}$$

$$M = \begin{bmatrix} A' & \mathbf{t}' \\ \mathbf{0}^T & 1 \end{bmatrix} \quad (43)$$

where,

$$A' = \frac{1}{\text{Det}A} \begin{bmatrix} a_1 a_4 + a_3 a_2 & 2a_2 a_4 \\ 2a_1 a_3 & a_1 a_4 + a_3 a_2 \end{bmatrix}, \quad \mathbf{t}' = \frac{1}{\text{Det}A} \mathbf{t}^T [\mathbf{1} - \text{diag}(s)] A.$$

■

Acknowledgment

This research was supported by the A.M.N. Foundation and by MUSCLE: Multimedia Understanding through Semantics, Computation and Learning, a European Network of Excellence funded by the EC 6th Framework IST Programme. T. Riklin-Raviv was also supported by the Yizhak and Chaya Weinstein Research Institute for Signal Processing.

REFERENCES

- [1] A.M. Bruckstein and D. Shaked. Skew-symmetry detection via invariant signatures. *Pattern Recognition*, 31(2):181–192, 1998.
- [2] V. Caselles, R. Kimmel, and G. Sapiro. Geodesic active contours. *International Journal of Computer Vision*, 22(1):61–79, Feb. 1997.
- [3] T.F. Chan and L.A. Vese. Active contours without edges. *IEEE Transactions on Image Processing*, 10(2):266–277, Feb. 2001.
- [4] Y. Chen, H.D. Tagare, S. Thiruvankadam, F. Huang, D. Wilson, K.S. Gopinath, R.W. Briggs, and E.A. Geiser. Using prior shapes in geometric active contours in a variational framework. *International Journal of Computer Vision*, 50(3):315–328, Dec. 2002.
- [5] H. Cornelius and G. Loy. Detecting rotational symmetry under affine projection. In *Proceedings of the International Conference on Pattern Recognition*, pages 292–295, 2006.
- [6] D. Cremers. Dynamical statistical shape priors for level set based tracking. *IEEE Transactions on Pattern Analysis and Machine Intelligence*, 28(8):1262–1273, August 2006.
- [7] D. Cremers, T. Kohlberger, and C. Schnorr. Shape statistics in kernel space for variational image segmentation. *Pattern Recognition*, 36(9):1929–1943, Sep. 2003.
- [8] D. Cremers, S. J. Osher, and S. Soatto. Kernel density estimation and intrinsic alignment for shape priors in level set segmentation. *International Journal of Computer Vision*, 69(3):335–351, September 2006.
- [9] D. Cremers and S. Soatto. A pseudo-distance for shape priors in level set segmentation. In *Workshop on Variational, Geometric and Level Set Methods in Computer Vision*, pages 169–176, 2003.
- [10] D. Cremers, N. Sochen, and C. Schnörr. Multiphase dynamic labeling for variational recognition-driven image segmentation. *International Journal of Computer Vision*, 66(1):67–81, January 2006.
- [11] A. Dervieux and F. Thomasset. A finite element method for the simulation of rayleigh-taylor instability. *Lecture Notes in Mathematics*, 771:145–158, 1979.
- [12] R. Fawcett, A. Zisserman, and J.M. Brady. Extracting structure from an affine view of a 3d point set with one or 2 bilateral symmetries. *Image and Vision Computing*, 12(9):615–622, November 1994.
- [13] J.M. Gauch and S.M. Pizer. The intensity axis of symmetry and its application to image segmentation. *IEEE Transactions on Pattern Analysis and Machine Intelligence*, 15(8):753–770, 1993.
- [14] A. Gupta, V.S.N. Prasad, and L.S. Davis. Extracting regions of symmetry. In *ICIP*, pages III: 133–136, 2005.
- [15] R. I. Hartley and A. Zisserman. *Multiple View Geometry in Computer Vision*. Cambridge University Press, 2nd edition, 2003.
- [16] W. Hong, Y. Yang, and Y. Ma. On symmetry and multiple view geometry: Structure, pose and calibration from single image. *International Journal of Computer Vision*, 60:241–265, 2004.
- [17] H. Ishikawa, D. Geiger, and R. Cole. Finding tree structures by grouping symmetries. In *Proceedings of the International Conference on Computer Vision*, pages 1132–1139, 2005.
- [18] K. Kanatani. Symmetry as a continuous feature: Comment. *IEEE Transactions on Pattern Analysis and Machine Intelligence*, 19(3):246–247, March 1997.
- [19] Y. Keller and Y. Shkolnisky. An algebraic approach to symmetry detection. In *Proceedings of the International Conference on Pattern Recognition*, pages III: 186–189, 2004.

- [20] S. Kichenassamy, A. Kumar, P.J. Olver, A. Tannenbaum, and A.J. Yezzi. Gradient flows and geometric active contour models. In *Proceedings of the International Conference on Computer Vision*, pages 810–815, 1995.
- [21] R. Kimmel. Fast edge integration. In S. Osher and N. Paragios, editors, *Geometric Level Set Methods in Imaging Vision and Graphics*. Springer-Verlag, 2003.
- [22] R. Kimmel and A.M. Bruckstein. Regularized laplacian zero crossings as optimal edge integrators. *International Journal of Computer Vision*, 53(3):225–243, 2003.
- [23] N. Kiryati and Y. Gofman. Detecting symmetry in grey level images: The global optimization approach. *International Journal of Computer Vision*, 29(1):29–45, 1998.
- [24] T. Kohlberger, D. Cremers, M. Rousson, and R. Ramaraj. 4d shape priors for level set segmentation of the left myocardium in SPECT sequences. In *Medical Image Computing and Computer-Assisted Intervention*, volume 4190, pages 92–100, October 2006.
- [25] A. Laird and J. Miller. Hierarchical symmetry segmentation. In *Proc. SPIE, Intelligent Robots and Computer Vision IX: Algorithms and Techniques*, volume 1381, pages 536–544, Feb. 1991.
- [26] M.E. Leventon, W.E.L. Grimson, and O. Faugeras. Statistical shape influence in geodesic active contours. In *IEEE Computer Society Conference on Computer Vision and Pattern Recognition*, volume I, pages 316–323, 2000.
- [27] T.L. Liu, D. Geiger, and A.L. Yuille. Segmenting by seeking the symmetry axis. In *Proceedings of the International Conference on Pattern Recognition*, pages 994–998, 1998.
- [28] L.M. Lorigo, O. Faugeras, Grimson W.E.L., R. Keriven, R. Kikinis, A. Nabavi, and C.F. Westin. Codimension two-geodesic active contours for the segmentation of tabular structures. In *IEEE Computer Society Conference on Computer Vision and Pattern Recognition*, pages 444–451, 2000.
- [29] G. Marola. On the detection of the axes of symmetry of symmetric and almost symmetric planar images. *IEEE Transactions on Pattern Analysis and Machine Intelligence*, 11(1):104–108, 1989.
- [30] D. Milner, S. Raz, H. Hel-Or, D. Keren, and E. Nevo. A new measure of symmetry and its application to classification of bifurcating structures. *Pattern Recognition*, 40:2237–2250, 2007.
- [31] D.P. Mukherjee, A. Zisserman, and J.M. Brady. Shape from symmetry– detecting and exploiting symmetry in affine images. *Phil. Trans. of the Royal Society of London*, 351:77–106, 1995. Series A.
- [32] D. Mumford and J. Shah. Optimal approximations by piecewise smooth functions and associated variational problems. *Communications on Pure and Applied Mathematics*, 42:577–684, 1989.
- [33] S. Osher and J.A. Sethian. Fronts propagating with curvature-dependent speed: Algorithms based on Hamilton-Jacobi formulations. *Journal of Computational Physics*, 79:12–49, 1988.
- [34] V.S.N Prasad and L. Davis. Detecting rotational symmetries. In *Proceedings of the International Conference on Computer Vision*, pages 954–961, 2005.
- [35] T. Riklin-Raviv, N. Kiryati, and N. Sochen. Unlevel-sets: Geometry and prior-based segmentation. In *Proceedings of the European Conference on Computer Vision*, volume 4, pages 50–61, 2004.
- [36] T. Riklin-Raviv, N. Kiryati, and N. Sochen. Prior-based segmentation by projective registration and level sets. In *Proceedings of the International Conference on Computer Vision*, volume I, pages 204–211, 2005.
- [37] T. Riklin-Raviv, N. Kiryati, and N. Sochen. Segmentation by level-sets and symmetry. In *IEEE Computer Society Conference on Computer Vision and Pattern Recognition*, volume 1, pages 1015–1022, June 2006.
- [38] T. Riklin-Raviv, N. Kiryati, and N. Sochen. Prior-based segmentation and shape registration in the presence of projective distortion. *International Journal of Computer Vision*, 72(3):309–328, May 2007.

- [39] T. Riklin-Raviv, N. Sochen, and N. Kiryati. Shape-based mutual segmentation. *International Journal of Computer Vision*, December 2007. Online Publication, DOI: 10.1007/s11263-007-0115-3.
- [40] T. Riklin-Raviv and N. Sochen, N.and Kiryati. Mutual segmentation with level-sets. In *The fifth IEEE computer society workshop on perceptual organization in computer vision*, June 2006.
- [41] M. Rousson and N. Paragios. Shape priors for level set representation. In *Proceedings of the European Conference on Computer Vision*, pages 78–92, 2002.
- [42] I. Shimshoni, Y. Moses, and M. Lindenbaum. Shape reconstruction of 3D bilaterally symmetric surfaces. *International Journal of Computer Vision*, 39(2):97–110, 2000.
- [43] J.S. Stahl and S. Wang. Globally optimal grouping for symmetric boundaries. In *IEEE Computer Society Conference on Computer Vision and Pattern Recognition*, volume 1, pages 1030–1037, June 2006.
- [44] S. Tari and J. Shah. Local symmetries of shapes in arbitrary dimension. In *Proceedings of the International Conference on Computer Vision*, pages 1123–1128, 1998.
- [45] D. Terzopoulos, A.P. Witkin, and M. Kass. Symmetry-seeking models and 3d object reconstruction. *International Journal of Computer Vision*, 1:211–221, 1987.
- [46] S. Thrun and B. Wegbreit. Shape from symmetry. In *Proceedings of the International Conference on Computer Vision*, pages 1824–1831, 2005.
- [47] A. Tsai, A. Yezzi, Jr., W.M. Wells, III, C. Tempany, D. Tucker, A. Fan, W.E.L. Grimson, and A.S. Willsky. A shape-based approach to the segmentation of medical imagery using level sets. *IEEE Transactions on Medical Imaging*, 22(2):137–154, Feb. 2003.
- [48] C.W. Tyler. *Human Symmetry Perception and Its Computational Analysis*. Lawrence Erlbaum Associates, 2002.
- [49] L.J. Van Gool, T. Moons, D. Ungureanu, and A. Oosterlinck. The characterization and detection of skewed symmetry. *Computer Vision and Image Understanding*, 61(1):138–150, January 1995.
- [50] L.J. Van Gool, T. Moons, D. Ungureanu, and E. Pauwels. Symmetry from shape and shape from symmetry. *International Journal of Robotics Research*, 14(5):407–424, October 1995.
- [51] A. Vasilevskiy and K. Siddiqi. Flux maximizing geometric flows. In *Proceedings of the International Conference on Computer Vision*, pages 149–154, 2001.
- [52] L.A. Vese and T.F. Chan. A multiphase level set framework for image segmentation using mumford and shah model. *International Journal of Computer Vision*, 50(3):271–293, 2002.
- [53] Y.A. Yang, K. Huang, S. Rao, W. Hong, and Y. Ma. Symmetry-based 3-d reconstruction from perspective images. *Computer Vision and Image Understanding*, 99:210–240, August 2005.
- [54] Y.A. Yang, S. Rao, K. Huang, W. Hong, and Y. Ma. Geometric segmentation of perspective images based on symmetry groups. In *Proceedings of the International Conference on Computer Vision*, volume 2, pages 1251–1258, 2003.
- [55] H. Zabrodsky, S. Peleg, and D. Avnir. Completion of occluded shapes using symmetry. In *IEEE Computer Society Conference on Computer Vision and Pattern Recognition*, pages 678–679, June 1993.
- [56] H. Zabrodsky, S. Peleg, and D. Avnir. Symmetry as a continuous feature. *IEEE Transactions on Pattern Analysis and Machine Intelligence*, 17(12):1154–1166, December 1995.
- [57] H. Zabrodsky and D. Weinshall. Using bilateral symmetry to improve 3d reconstruction from image sequences. *Computer Vision and Image Understanding*, 67:48–57, 1997.